ISSN 1070-3632, Russian Journal of General Chemistry, 2014, Vol. 84, No. 13, pp. 2499–2515. © Pleiades Publishing, Ltd., 2014.
Original Russian Text © A.Yu. Kudeyarova, T.V. Alekseeva, E.I. Elfimov, 2013, published in Ekologicheskaya Khimiya, 2013, Vol. 22, No. 4, pp. 215–233.

Conditions and Mechanisms of the Transformation of Gibbsite into Taranakite in Phosphate Solutions

A. Yu. Kudeyarova, T. V. Alekseeva, and E. I. Elfimov

Institute of Physicochemical and Biological Problems of Soil Sciences, Russian Academy of Sciences, ul. Institutskaya 2, Pushchino, Moscow oblast, 142290 Russia
e-mail: vnikolaevich2001@mail.ru

Received December 15, 2013

Abstract—Structural changes in gibbsite (an Al-containing soil mineral) in $NH_4H_2PO_4$ solutions of different concentrations (from 10^{-6} to 2 M) were studied. As the concentration of the solution was increased, increasing release of aluminum from gibbsite to the liquid phase was observed along with binding of phosphate anions. The resulting soluble complex (aluminophosphate) anions were responsible for gibbsite dissolution. The most intense gibbsite dissolution occurred in 1 M and 2 M phosphate solutions. Evidence was obtained to show that this phenomenon is associated with the formation of aluminum complexes with pyro(poly)phosphate ligands. Along with intense gibbsite dissolution, a phosphate mineral (ammonium taranakite) formed, which was confirmed instrumentally. The key role of anionic aluminum pyro(poly)phosphate complexes in the formation of taranakite crystals was revealed. Sequential changes in the ligands in the complexes, associated with increasing phosphate loading, are discussed.

Keywords: gibbsite, chemisorption of phosphate anions, dissolution of gibbsite, complex (aluminophosphate) anions, pyro(poly)phosphate ligands, formation of ammonium taranakite

DOI: 10.1134/S1070363214130039

INTRODUCTION

The ability of soil metal compounds to bind (chemisorb) phosphate anions is well known, but products that form at varied phosphate loadings on sorbents have scarcely been studied. Over the past decades enhanced phosphorus migration processes have been observed, but the opinion that phosphate anions are strongly retained on the surface of Al- and Fe-containing sorbents which fulfill a barrier function in acid soils still remains very common. This opinion is based on the possibility of formation of binuclear metal phosphate complexes, where one phosphate anion is coordinated to two surface metal (Me) atoms. Such complexes are generally formed at low concentrations of P_2O_5 in solutions [1], which are observed in natural soils but not in soils overloaded with phosphates due to the use of phosphate fertilizers.

The coordination of phosphate anions (electron donors) to positively charged metal atoms (electron acceptors) in natural surface sorbent complexes is accompanied by cleavage of the metal–ligand bonds with release of the ligands into the solution. In natural mineral sorbents, the most facile substitution in surface complexes is characteristic of aquo and hydroxo ligands. In essence, this is an initial stage of the transformation of sorbents [2].

Increasing concentration of the phosphate solution increases the probability of Me–OH–Me bond cleavage, which leads to elimination of some structural fragments of the polymeric molecules [3] and facilitates formation of mononuclear complexes of the general formula $Me(X_yZ_n)$ (where Me = Al^{3+}, Fe^{3+}; X = $H_2PO_4^-$, HPO_4^{2-}, PO_4^{3-}; Z = H_2O, OH^-) typical of simple phosphate salts. These are mixed-ligand complexes, as they contain phosphate, as well as aquo and hydroxo ligands. The coating formed by the $Me(X_yZ_n)$ complexes on the surface of sorbents is amorphous by X-ray diffraction (XRD) [3–6].

Coordination of a new ligand is always accompanied by electron density redistribution in the complex [7]. This process reveals itself in the

deprotonation of the phosphate ligand, leading to an increase of the dentacity of the latter [1]. Thus, the $H_2PO_4^-$ anion coordinates to metal by one O atom, and the HPO_4^{2-} anion, by two O atoms. If a metal phosphate complex contains two bidentate ligands, it bears a negative charge [8–11] and has a cyclic (chelate) structure:

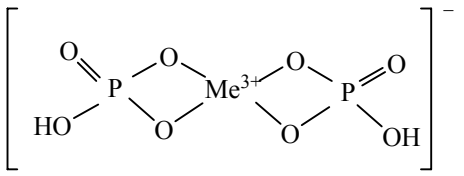

Negatively charged surfaces of sorbents strongly bind cations from the solution [1, 3, 9, 11–13].

Negatively charged Me^{3+}-phosphate complexes should be considered as anions of metallophosphoric acids [14–17], i.e. as anions of a higher order than anions of a normal phosphoric acid. A peculiar feature of complex anions is that, as their charge increases, they show increasing solubility and increasing tendency for substitution of strongly bound ligands, including phosphate ligands. This feature is responsible for the incongruent dissolution of phosphorus compounds in phosphate solutions, which involves consecutive formation of increasingly complex soluble and solid products.

Previous studies [1, 2, 18, 19] showed that the anionic metal phosphate complexes formed by binding of phosphate anions to sorbent compounds in acid soils can pass into the liquid phase. The solid products in phosphorus-enriched soils are mostly represented [5, 19–21] by double (triple) salts of metallophosphoric acids of the general formula $Me^1_b[MeX]$, where $Me^1 = Ca^{2+}$, K^+, Na^+, NH_4^+ , and other cations; $Me = Al^{3+}$, Fe^{3+}; and $X = HPO_4^{2-}$, PO_4^{3-}. Such salts are also present in natural soils [22, 23], especially soils formed from rocks enriched with lithogenic or biogenic phosphates [21, 24].

At the sites of contact of biogenic phosphates (guano, bones, and other organic matter) with magmatic and sedimentary rocks, such complex phosphate salts as taranakite–leucophosphite series minerals of the general (arbitrary) formula $(NH_4^+, K^+)_3(Al, Fe^{3+})_5 \cdot (HPO_4)_6(PO_4)_2 \cdot 18H_2O$ are formed [25–28]. Theoretically, taranakite should contain aluminum, and leucophosphite should contain iron. In view of the specific nature of the anionic part of ammonium taranakite, we can present the latter as the ammonium salt of aluminophosphoric acid $(NH_4^+)_3[Al_5(HPO_4)_6 \cdot (PO_4)_2]^{3-} \cdot 18H_2O$. The P/Al ratio in ammonium taranakite is 1.83, whereas the respective ratio in the simple aluminophosphate mineral variscite ($AlPO_4 \cdot 2H_2O$) is 1.15. The high P/Al ratio gives evidence showing that taranakite formation is associated with the formation of anionic aluminophosphate complexes, such as $[Al(HPO_4)_2]^-$, $[Al(HPO_4)(PO_4)]^{2-}$, and $[Al(PO_4)_2]^{3-}$, which contain more phosphorus that positively charged or neutral complexes corresponding to simple phosphate salts: $[Al(H_2PO_4)]^{2+}$, $[Al(HPO_4)]^+$, $[Al(PO_4)]^0$.

In model experiments with Al-containing soil sorbents, the researchers (in view of the mentioned binding of cations from the solution), did not obtain anyinstrumental evidence of taranakite formation. This result is apparently explained by the fact that the phosphate solutions used in their experiments had fairly low concentrations (normally, $\leq 10^{-3}$–10^{-2} M), as well as too short solution−sorbent contact times. The aforesaid points to the necessity of a more detailed research into structural changes in Al-containing soil sorbents under varied phosphate loadings. From our viewpoint of particular importance is to study the effect of abnormally high phosphate loadings, because quite scarce information on this subject is available in the literature. At the same time, there is a possibility of the local sites in soils overphosphatized due to human activities, where the phosphate loading of sorbents is higher than loadings characteristic of the surrounding soil by several orders of magnitude [19].

In the present work we set ourselves the goals (1) to study the structural changes in the gibbsite mineral exposed to phosphate solutions with concentrations close to those characteristic of both natural soil solutions and localized solutions in the reaction zones of phosphorus fertilizer granules and (2) to reveal the conditions and mechanisms of the transformation of gibbsite to taranakite.

EXPERIMENTAL

Aluminum hydroxide with the formula $Al(OH)_3$ was used in the experiments. Its XRD pattern corresponded to gibbsite [29]. Gibbsite (a natural sorbent in acid soils) is one of the final products of rock weathering in the process of soil formation. The Al atom in the gibbsite crystal has the coordination number of 6 and octahedral environment of OH ligands. The crystals generally have a pseudo-

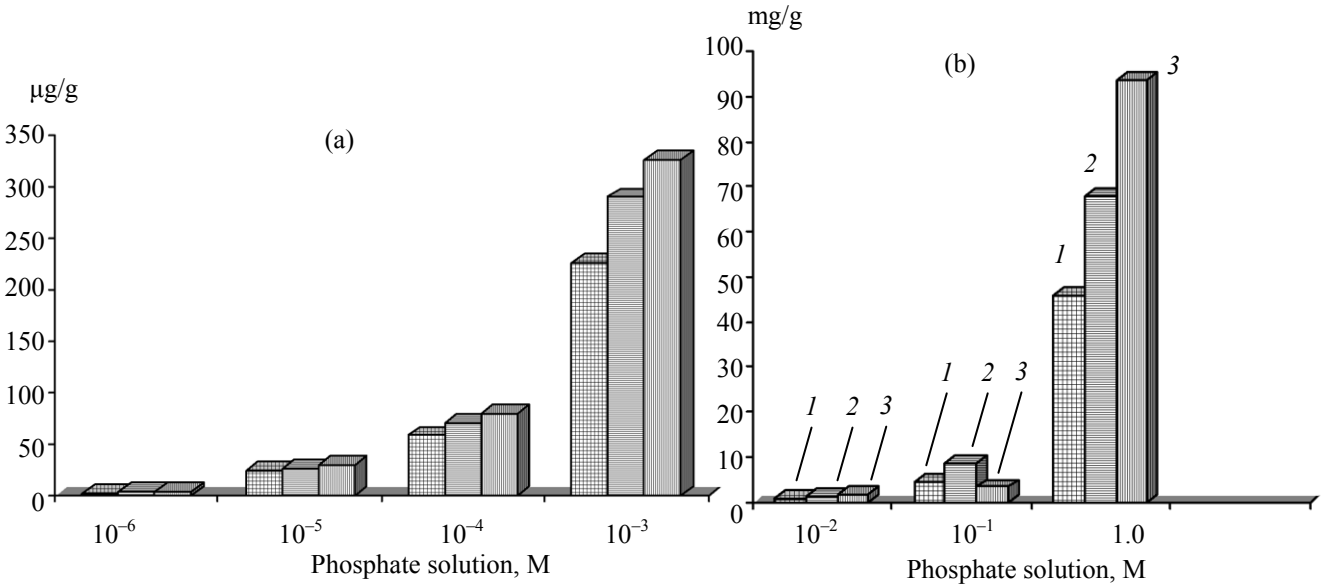

Fig. 1. Binding of phosphate anions from $NH_4H_2PO_4$ solutions by gibbsite. Phosphate concentration: (a) μg P/g gibbsite and (b) mg P/g gibbsite. Treatment time: (*1*) 1 day, (*2*) 10 days, and (*3*) 2 months.

hexagonal cross-section, and an important role in their formation belongs to hydrogen bonds.

Distilled water (control) or a solution of $NH_4H_2PO_4$ (*c* 10^{-6}, 10^{-5}, 10^{-4}, 10^{-3}, 10^{-2}, 10^{-1}, 1 M, 2 M P) were poured onto $Al(OH)_3$ powder (100 mL : 1 g). The initial pH value in the $Al(OH)_3$–H_2O and $Al(OH)_3$–$NH_4H_2PO_4$–H_2O systems was varied in the range 4.56–4.61. Suspensions were shaken for 2 h and left to stand at room temperature for 1 day, 10 days, and 2 months; every day they were shaken for 1 min. Filtrates of the suspensions (the liquid phase of the systems) were analyzed for phosphorus and aluminum on an Optima 5300 DV atomic emission spectrometer (USA). Filtrates with high phosphorus concentrations were diluted with distilled water to *c* 10^{-3} M P before analysis. Sample preparation for the analysis for P and Al involved 10-min boiling of filtrate aliquots with $HCl_{1.19}$ to destroy the aluminophosphate complexes [30]. From the difference in the P concentrations in the initial solutions and liquid phases of the $Al(OH)_3$–$NH_4H_2PO_4$–H_2O systems we calculated the amounts of phosphates bound by gibbsite. The analytical results presented in the paper are averaged over three runs. The deviations from the average values were not greater than 4% for phosphorus and 6% for aluminum.

The electronic absorption spectra of the liquid phase of the $Al(OH)_3$–H_2O and $Al(OH)_3$–$NH_4H_2PO_4$–H_2O systems were registered on a Hitachi-557 spectrometer (Japan) in a 20-mm cell; the etalons were water and the liquid phase of the control system $Al(OH)_3$–H_2O, respectively.

The solid products of the phosphate treatment of aluminum hydroxide, as well as the precipitate formed in the liquid phase of the system with the initial concentration 1 M P (after 3-month storage at room temperature in the dark) were separated, washed with H_2O, and dried in air, after which they were analyzed by instrumental methods. X-ray diffraction analysis was performed on a DRON-3 instrument (Co anode). The structural transformations of gibbsite in phosphate solutions were traced on a TESKAN VEGA3 scanning electron microscope equipped with an Oxford Instruments X-Max 50 silicon drift EDS system. The IR spectra were obtained on a Nicolet 6700 FTIR instrument at 4000–400 and 1000–375 cm^{-1} in KBr pellets (200 mg, including 1 mg sample).

RESULTS AND DISCUSSION

Figure 1 shows that the amounts of gibbsite-bound phosphate anions are directly related to the concentration of the phosphate solution. In the case of 10^{-6}–10^{-4} M phosphate solutions (characteristic of natural soil solutions), all phosphate was found to be bound by gibbsite after 2-month treatment. The fact that the binding process occurred fairly slowly is likely to be explained by the crystal structure of gibbsite. Gibbsite crystals can be considered as polynuclear

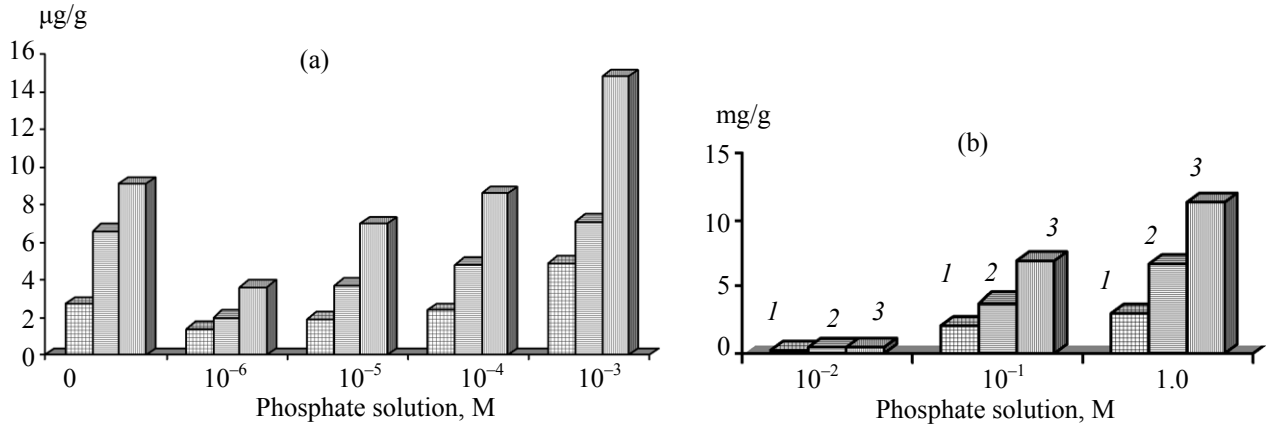

Fig. 2. Release of aluminum into the liquid phase of gibbsite–phosphate solution systems. Concentration: (a) μg Al/g gibbsite and (b) mg Al/g gibbsite. Treatment time: (*1*) 1 day, (*2*) 10 days, and (*3*) 2 months.

complexes, where Al atoms are strongly bridged by OH ligands. The most susceptible to substitution for phosphate anions are, first of all, aquo and hydroxo ligands of the corresponding aluminum complexes on defective crystal surfaces.

According to data in Fig. 2, the liquid phase of the systems with 10^{-6}–10^{-4} M phosphate solution contained less aluminum (as a component of complexes destroyed by acid thermolysis) than the control system gibbsite–water. The difference electronic absorption spectra (Fig. 3) revealed the same relation for hygroscopic aluminum complexes in the corresponding phosphate systems. Our results gave evidence showing that phosphate anions from solutions with concentrations close to natural (c 10^{-6}–10^{-4} M) are strongly bound in aluminophosphate complexes on the gibbsite surface.

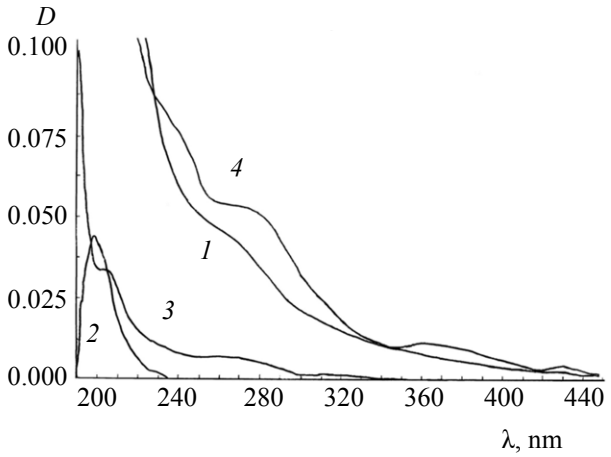

Fig. 3. Electronic absorption spectra of the liquid phase of gibbsite–phosphate solution systems after 1-day treatment. Phosphate concentration, M: (*1*) no phosphate, control (reference H_2O), (*2*) 10^{-6}, (*3*) 10^{-4}, and (*4*) 1.0 (references in 2, 3, and 4 are the liquid phase of the control system).

As the concentration of the solution increases, more and more aluminum released into the liquid phase as compared to the amount of aluminum in the liquid phase of the control system (Fig. 2). The release of Al into the liquid phase from the aluminophosphate complexes destroyed by acid hydrolysis was first noted in the case of 10^{-3} M phosphate solutions, and it progresssively enhanced in going to 10^{-1} M, and, especially 1 M phosphate solutions. The difference electronic absorption spectrum of the liquid phase of a 1 M phosphate solution (Fig. 3) revealed additional absorption bands (compared to the control system), which may be assigned to phosphate and aluminophosphate anions. It was found that the contribution of soluble aluminophosphate complexes in the total binding of phosphates by gibbsite increased with increasing concentration of the phosphate solution.

The XRD patterns (not shown) of the products of 1- and 10-day, as well as 2-month treatment of gibbsite with 10^{-3}–10^{-1} M phosphate solutions showed no additional peaks compared with the control gibbsite. The detection of aluminum in the liquid phase (Fig. 2) suggests dissolution of X-ray amorphous aluminophosphates in the phosphate solution. Evidence for the dissolution of the phosphatized layer of gibbsite is also provided by the fact that the phosphorus content in the solid phase decreased (Fig. 1) as the time of phosphate treatment with a 10^{-1} M phosphate solution was increased from 10 days to 2 months. This finding implies that a considerable part of the phosphorus

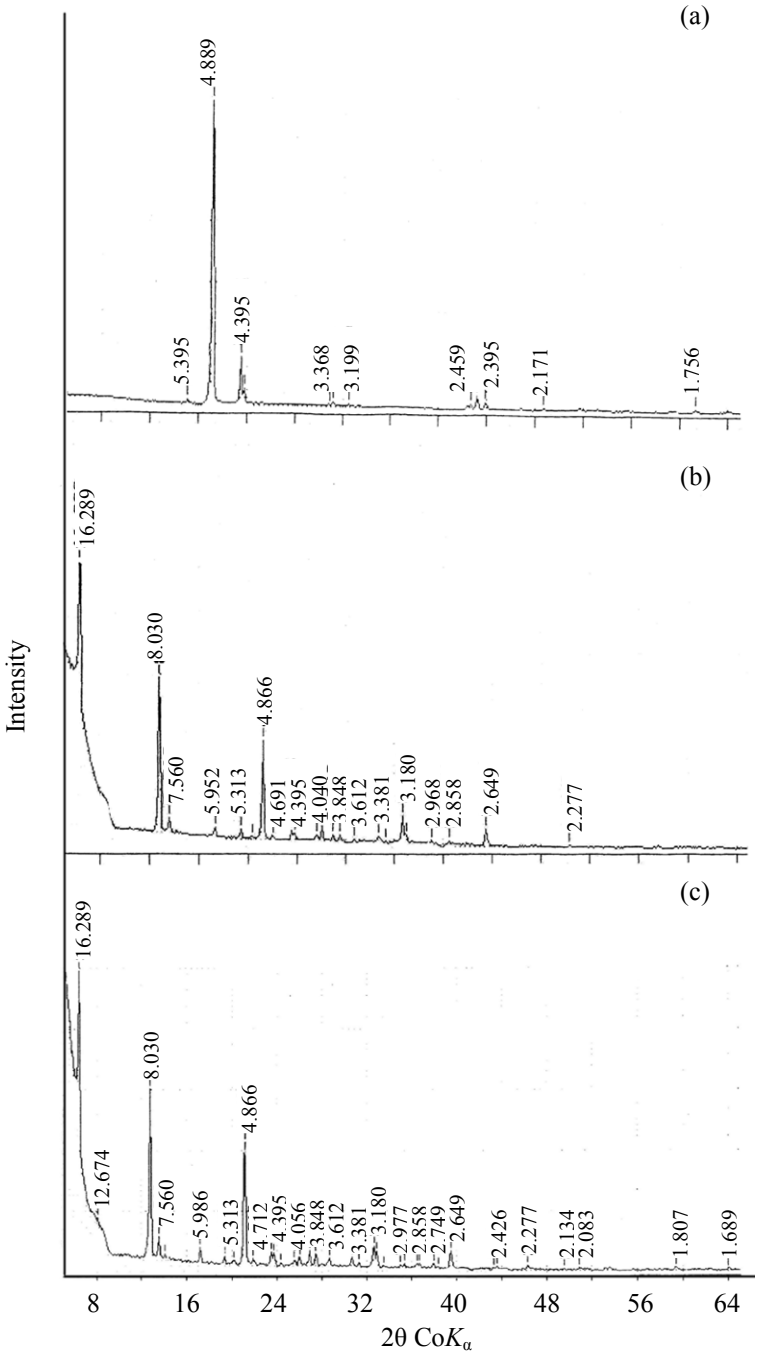

Fig. 4. X-ray diffraction patterns of gibbsite and products of its 2-month treatment with: (a) water (control), (b) 1 M phosphate solution, and (c) 2 M phosphate solution.

bound by gibbsite has passed into the solution. Consequently, the structure and properties of the previously formed aluminophosphate complexes changed, probably, as a result of addition of one more phosphate ligand which increased a negative charge of the complexes.

It can be suggested that the complex anions formed under a high phosphate loading of gibbsite catalyzed structural transformations of gibbsite (Fig. 4a) in the systems with 1 M and 2 M phosphate solutions (Figs. 4b and 4c). The XRD pattern of the product of 2-month treatment of gibbsite with a 1 M phosphate solution (Fig. 4b) shows no peaks characteristic of this mineral [29], except for one (4.395 Å), but it has a lower intensity. The peaks at 16.289, 8.030, and 7.560 Å with intensities of 99.9, 100.0, and 9.4% are charac-

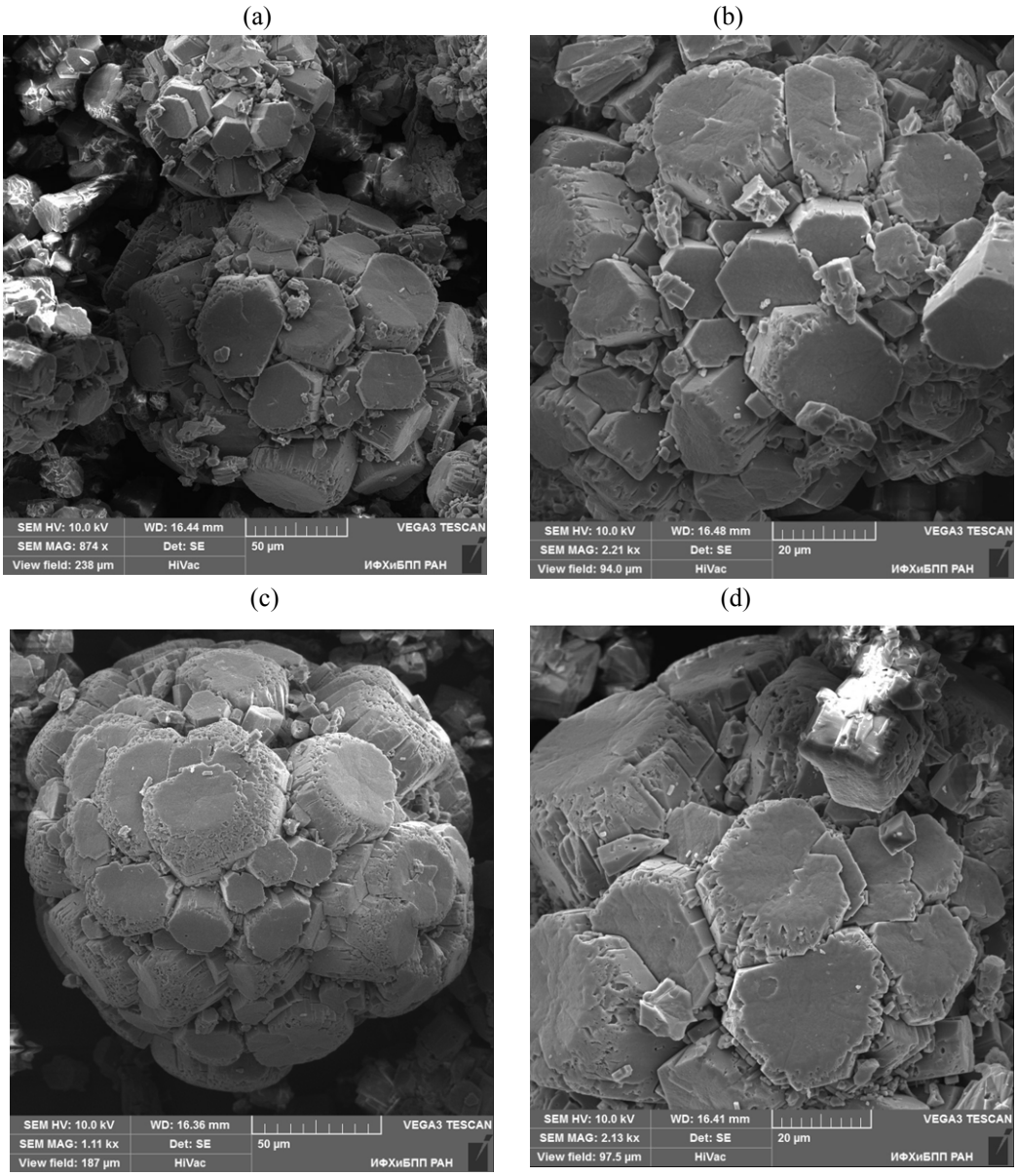

Fig. 5. Electronic images of gibbsite after 2-month treatment with (a, b) water [magnification: (a) × 874 and (b) × 2210], and (c, d) 10^{-3} M phosphate solution [(c) × 1110 and (d) × 2130].

teristic of ammonium taranakite $(NH_4)_3H_6Al_5(PO_4)_8 \cdot 18H_2O$ [31]. The other peaks in the XRD pattern (except for those at 5.313 и 4.866 Å), too, are characteristic of this mineral.

The XRD pattern of the product of 2-month treatment of gibbsite with a 2 M phosphate solution (Fig. 4c) has the same peaks as the XRD bound by pattern of the product of treatment with a 1 M phosphate solution (Fig. 4b), as well as additional peaks at 5.952, 4.691, and 4.040 Å, which, too, belong to ammonium taranakite. Moreover, the XRD pattern (Fig. 4c) shows peaks characteristic of pyro(poly)-phosphoric acids, rather than of taranakite [31]. For example, the peaks at 5.313, 4.866, and 3.106 Å (the first two peaks are also observed in the XRD pattern of the product formed in the 1 M P system) are characteristic of the pyrophosphate salt $(NH_4)_3HP_2O_7$.

Structural transformations of gibbsite during its 2-month treatment with phosphate solutions were studied by scanning electron microscopy (Figs. 5–7). Figure 5a shows that the gibbsite crystals in the control system (with H_2O, without P) were initially grouped into ball-

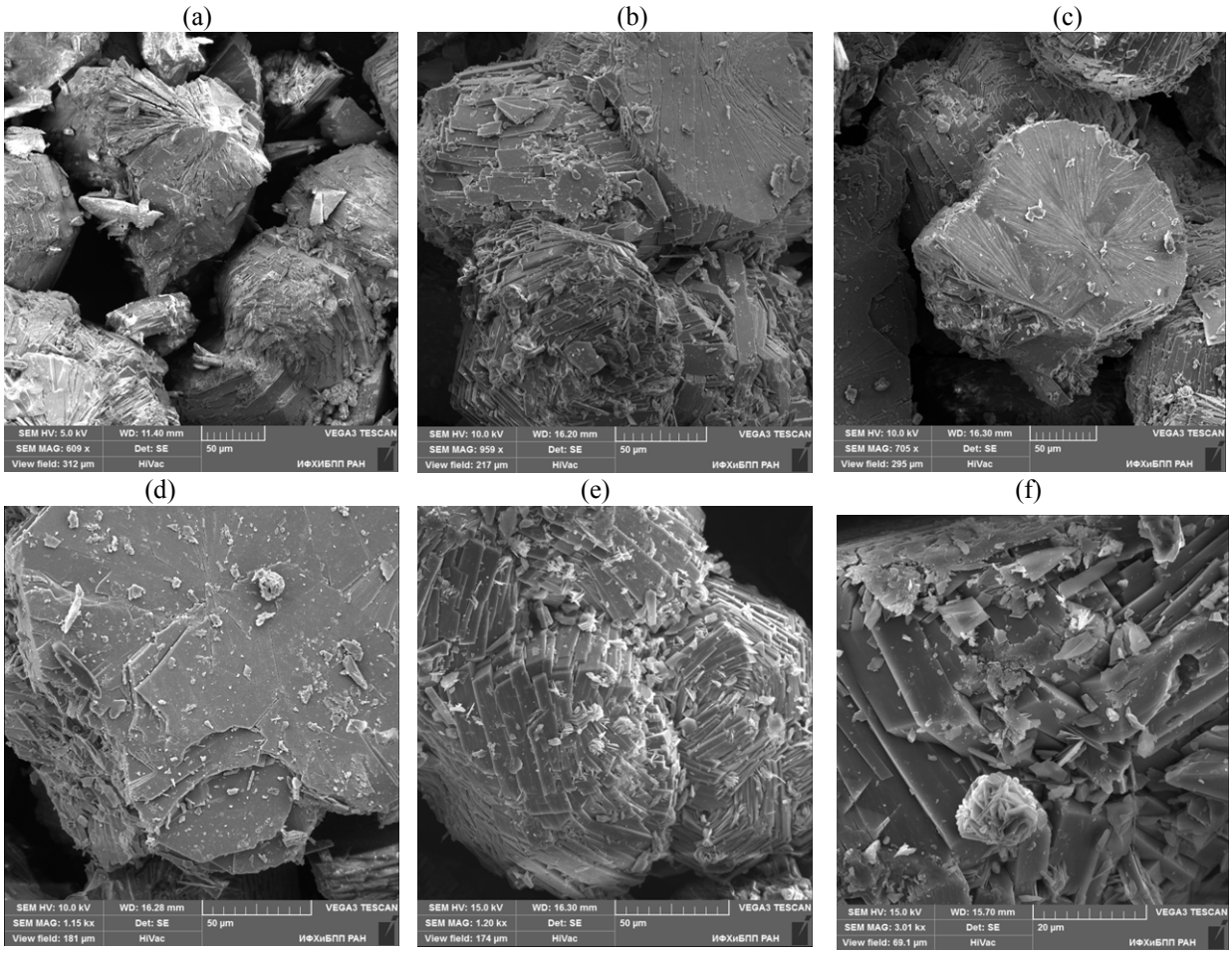

Fig. 6. Electronic images of the product of 2-month treatment of gibbsite with a 1 M phosphate solution. Magnification: (a) × 609, (b) × 959, (c) × 705, (d) × 1150, (e) × 1200, and (f) × 3010.

shaped aggregates about 170 μm in size. Individual crystals (Fig. 5b) had different peripheral defects like shares, cleavages, and pittings (pores, grooves, etc.), as well as different sizes (25−15 and < 1 μm). Such crystal defects might result for hydrolysis that formed anionic hydroxo complexes of aluminum [32]: $Al(OH)_3 + H_2O = [Al(OH)_4]^- + H^+$. The presence of the anionic complexes in the liquid phase of the gibbsite–H_2O system is confirmed by the electronic absorption spectrum (Fig. 3, curve *1*) and the increasing amount of aluminum in the liquid phase (Fig. 2).

The liquid phase of gibbsite treated for 2 months with a 10^{-3} M phosphate solution contained more aluminum than control (Fig. 2). Accordingly, in Figs. 5c and 5d we observed slightly more expressed peripheral crystal defects, even though the shapes of crystals, as well as the shape of aggregates as a whole, did not change.

After 2-month treatment of gibbsite with a 1 M phosphate solution, the shape of aggregates radically changed (Figs. 6a and 6b). As judged from the size of aggregates, they preserved integrity (no splitting into component crystals did not occur), but their "smoothed," flaked surface of the aggregates suggested dissolution of the phosphatized top layer. This process is illustrated by an example of an individual aggregate (Fig. 6c), whose bottom part shows a well-defined flaking (Fig. 6d). Evidence for the dissolution of the phosphatized gibbsite surface comes from a high concentration of aluminum in the liquid phase of the corresponding system (Fig. 2). Along with dissolution, a new rosette-shaped bulky phase formed (Figs. 6e and 6f).

Spectrometric microanalysis (Table 1) of the surface layers of aggregates and their flaky fragments (Figs. 6a–6d), as well as bulky formations (rosettes) at

Table 1. Composition of the transformation products of gibbsite in 1 M (Fig. 6) and 2 M (Fig. 7) phosphate solutions

Figure no.	Element	Content, %	Ratio		Figure no.	Element	Content, %	Ratio	
			P/Al	P/N				P/Al	P/N
6a	P Al N	18.41 9.91 3.34	1.86	5.51	–	–	–	–	–
6b	P Al N	18.30 9.84 3.71	1.86	4.93	7b	P Al N	19.03 10.39 3.40	1.83	5.60
6c	P Al N	20.89 10.68 4.28	1.96	4.88	7c	P Al N	22.02 10.25 4.51	2.15	4.88
6d	P Al N	22.20 10.52 5.03	2.11	4.41	7d	P Al N	25.80 11.26 6.04	2.29	4.27
6e, 6f (rosettes)	P Al N	22.72 10.21 5.30	2.23	4.29	7e (rosettes)	P Al N	28.91 10.75 6.92	2.69	4.18

Table 2. Composition of some aluminophosphate anions and ammonium phosphate salts

Anion, salt	Element	Content, %	Ratio	
			P/Al	P/N
$[Al(HPO_4)_2]^-$	P	29.22	2.37	
	Al	12.32		
$[Al(HPO_4)(PO_4)]^{2-}$	P	28.44	2.30	
	Al	12.38		
$[Al(PO_4)_2]^{3-}$	P	28.57	2.29	
	Al	12.44		
$[Al(HPO_4)(P_2O_7)]^{3-}$	P	31.31	3.44	
	Al	9.09		
$(NH_4)_3[Al_5(HPO_4)_6(PO_4)_2 \cdot 18H_2O$ (ammonium taranakite)	P	19.39	1.83	5.91
	Al	10.60		
	N	3.28		
$NH_4H_2PO_4$	P	26.96		2.22
	N	12.17		
$(NH_4)_3HP_2O_7$	P	27.07		1.48
	N	18.34		
$(NH_4)_4P_2O_7$	P	25.20		1.11
	N	22.76		

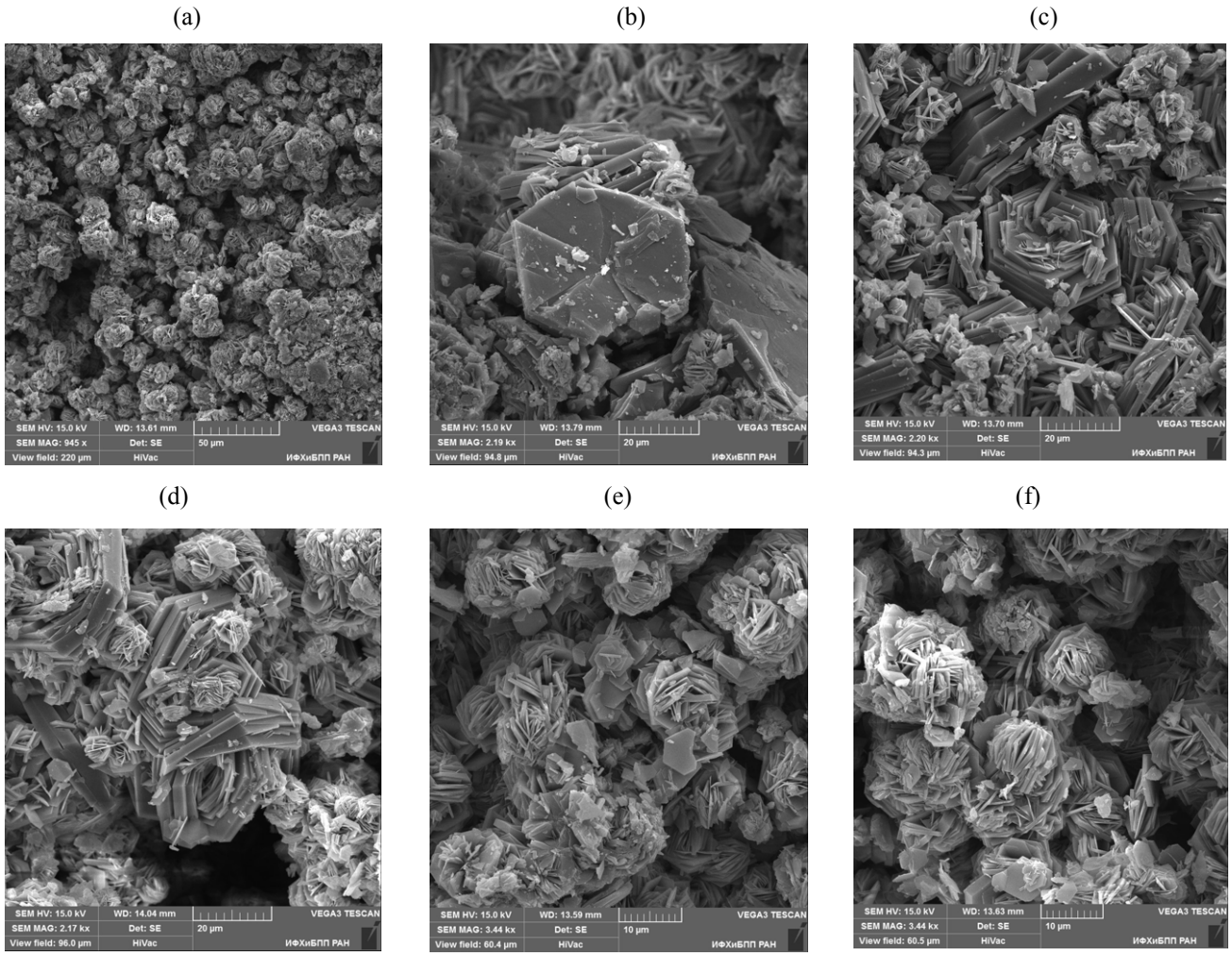

Fig. 7. Electronic images of the product of 2-month treatment of gibbsite with a 2 M phosphate solution. Magnification: (a) × 945, (b) × 2190, (c) × 2200, (d) × 2170, (e) × 3440, and (f) × 3440.

cracks in the surface (Figs. 6e and 6f) showed that the samples differ in elemental compositions: The most essential distinctions are in phosphorus contents. Along with P and Al, the composition also included nitrogen whose content was directly related to the content of phosphorus.

The close contents of P, Al, and N (Table 1) were observed both on the surface of the aggregate shown in Fig. 6a (top, center) and on flake surface (Fig. 6b, left). As judged from the P/Al ratio equal to 1.86 and the content of nitrogen, the composition of the surface layers is close to that of ammonium taranakite (Table 2). The P/Al ratios in the surface layers of the aggregate shown in Fig. 6c and its dissolved part (Fig. 6d) are 1.96 and 2.11, that is higher than the respective value (1.83) for taranakite (Tables 1, 2). The highest P/Al ratio (2.23) was found in the "rosette" phase (Fig. 6e and 6f). This phase contained more phosphorus (22.72%) and nitrogen (5.30%) than the surface layers (Table 1). The higher contents of P and N compared to the theoretical values (19.39% P and 3.28% N) for ammonium taranakite with a standard chemical formula (Table 2), points to a higher negative charge of the aluminophosphate complexes forming the bulk phase of rosettes on phosphatized cracks in surface layers (Figs. 6e and 6f). Such complexes might penetrate into aggregates with the solution through surface cracks.

Apparently, the in-depth penetration of complex anions is responsible for the complete destruction of

gibbsite aggregates to form a new phase (Fig. 7a), after 2-month treatment with a 2 M phosphate solution. The new phase mostly consisted of small (5−15 μm) discrete formations. In the right bottom corner of the picture one can note, among fragments of the partly destroyed treatment product, a hexagonal formation. At a higher magnification (Fig. 7b) it becomes evident that this is a crystal having cracks in the surface layer and a rosette phase on the edges. The P, Al, and N contents and P/Al ratio in the surface layer of the crystal (Table 1) were coincident with the theoretical values for ammonium taranakite (Table 2).

The cross-sectional dimension of the crystal (Fig. 7b) is 42 μm, i.e. this crystal is much larger than similarly shaped gibbsite crystals (Fig. 5b). From this it follows that this large crystal was formed by the transformation of the whole aggregate of gibbsite crystals. It should be noted that a similarly shaped and sized crystal of ammonium taranakite and, too, having bulk secondary formations on the surface, was ob-tained from the reaction mixture with a 1 : 1.4 : 0.7 : 62 $Al_2O_3/P_2O_5/NH_4/H_2O$ molar ratio but under heating at 70°C [33].

The fact that the large taranakite crystal (Figs. 7a and 7b) is surrounded by smaller formations allows it to be considered as an intermediate product subject to further transformations in a 2 M phosphate solution. Figures 7b–7d allows us to trace the sequence of transformations involving crystal delamination and layer thinning. The dissolution process was apparently catalyzed by the incorporated complex anions. In the course of dissolution, the contents of phosphorus and nitrogen in the solid product increased but the content of aluminum remained virtually invariable (Table 1). In the end small structures were formed that have the shape of balls transforming into rosettes, which is well seen on their magnification (Figs. 7e and 7f).

According to data in Table 1, the rosette structures had especially high phosphorus and nitrogen contents (28.91 and 6.92%, respectively). The P/Al ratio in the rosettes (2.69) was higher than in taranakite (1.83) with the anionic part representing a polynuclear aluminophosphate complex with the charge –3, which contains 2 types of bi(poly)dentate orthophosphate ligands (HPO_4^{2-} and PO_4^{3-}), as well as in mononuclear complexes with the same ligands: $[Al(HPO_4)_2]^-$, $[Al(HPO_4)(PO_4)]^{2-}$, and $[Al(PO_4)_2]^{3-}$ (2.37, 2.30, and 2.30, respectively, Table 2).

It can be suggested that the transformation of the large crystal in a 2 M phosphate solution into rosette-shaped structures (Figs. 7e and 7f) is associated with the formation of aluminophosphate complexes with pyro(poly)phosphate ligands, like, for example, in the complex $[Al(HPO_4)(P_2O_7)]^{3-}$ (P/Al 3.44) (Table 2). Evidence can be found in the XRD pattern (Fig. 4c) and IR spectra (Figs. 8 and 9) of the product of 2-month treatment of gibbsite with a 2 M phosphate solution, which show, respectively, peaks and absorption bands assignable to condensed phosphates.

The ESM images (Figs. 7e and 7f) show that the rosette-shaped structures, too, were not stable in the phosphate solution, as seen from the fact that these structures "eject" small (cross-sectional dimension ca. 8 μm) hexagonal plates (Fig. 7e) which accumulate among the products formed in the system treated with a 2 M phosphate solution (Fig. 7f, bottom). Similarly shaped and sized ammonium taranakite crystals were obtained by heating a mixture of aqueous solutions of $Al(H_2PO_4)_3$ and NH_4OH at 90°C [13]. When increasing amounts of ammonium citrate were added to the mixture, taranakite crystals decreased in size and changed shape from hexagonal to disk-like.

Changes in the bond system of gibbsite under varied phosphate loadings were studied by IR spectroscopy. The most characteristic vibrational bands in the IR spectrum of gibbsite in the control system (H_2O, no phosphate) (Fig. 8, curve *1*) belonged to O–H (4000–2500 cm^{-1}) and Al–O (<1000 cm^{-1}) bonds. The absorption bands in the range below 420 cm^{-1} were assigned to metal−oxygen bonds in anionic complexes [34].

The spectral data (spectra are not shown) revealed no changes in the bond system of gibbsite (4000–400 cm^{-1}) after 2-month treatment with 10^{-6}–10^{-4} M phosphate solutions. Treatment of gibbsite with a 10^{-1} M phosphate solution (Fig. 8a) scarcely affected the positions of the principal absorption bands in the range 4000–500 cm^{-1} but decreased their intensity due to substitution of the OH groups and formation of soluble aluminophosphate complexes. A strongly decreased intensity of all absorption bands in the studied spectral range was noted already after 1-day treatment of gibbsite with a 1 M phosphate solution (Fig. 8a).

According to the IR spectra (Fig. 8b), after 2-month treatment with 1 M and 2 M phosphate solutions gibbsite almost completely transformed into a new phosphate phase. Hydroxyl absorption (with a much decreased intensity) in remaining gibbsite particles is observed in the range above 3300 cm^{-1}. The formation

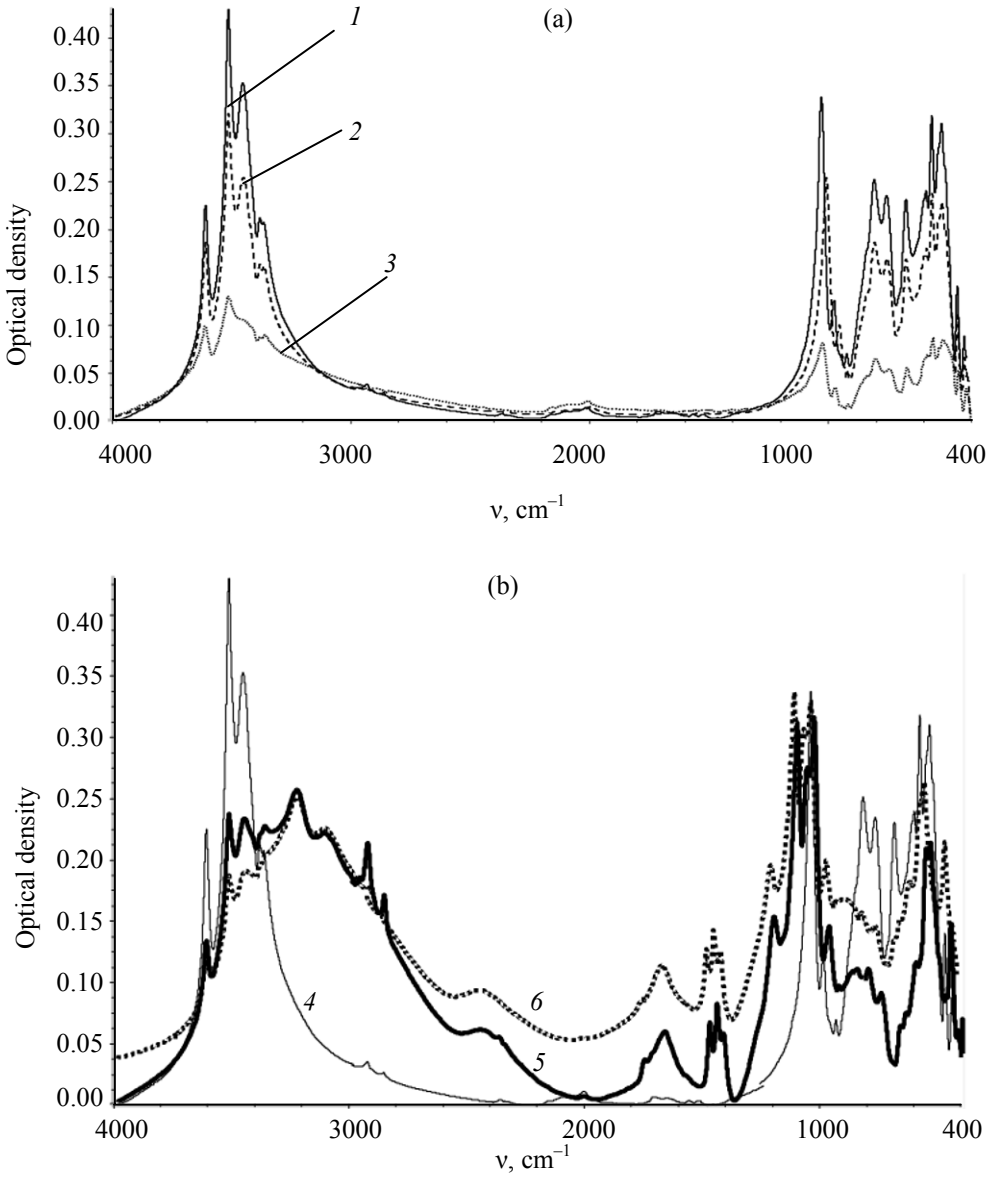

Fig. 8. IR spectra of gibbsite and products of its treatment with phosphate solutions. (a): (*1*) gibbsite, H_2O, 2 months (control); phosphate concentration, M: (*2*) 10^{-1} (2 months) and (*3*) 1 (1 day); (b): (*4*) gibbsite, H_2O, 2 months (control); phosphate concentration, M: (*5*) 1 (2 months) and (*6*) 2 (2 months).

of a new phosphate phase is evidenced by the presence of absorption bands of P-containing groups in the IR spectra. The two bands near 1463 and 1432 cm^{-1} can be assigned to free P=O groups in, apparently, ligands of two types (ortho- and polyphosphate) in aluminum complexes, and the band near 1190 cm^{-1} is assignable to hydrogen-bonded P=O groups [14]. The broad band peaking at 2430 cm^{-1} is associated with exceptionally strong chelate metal complexes with a strong intramolecular hydrogen bond. This bond involves the P(O)OH group which has a proton-donor OH group at the P=O phosphorus atom, and the P=O oxygen acts as a proton acceptor [14, 34]. The newly formed intermolecular hydrogen bonds involving OH and NH groups absorb in the range 3300–2500 cm^{-1}. Thus, the presence of an absorption band near 3129 cm^{-1} suggests the involvement of the NH groups of the NH_4^+ ions in such bonds. The stretching and deformation vibrations of the NH_4^+ ions themselves are observed at 1430 and 1655 cm^{-1} [34].

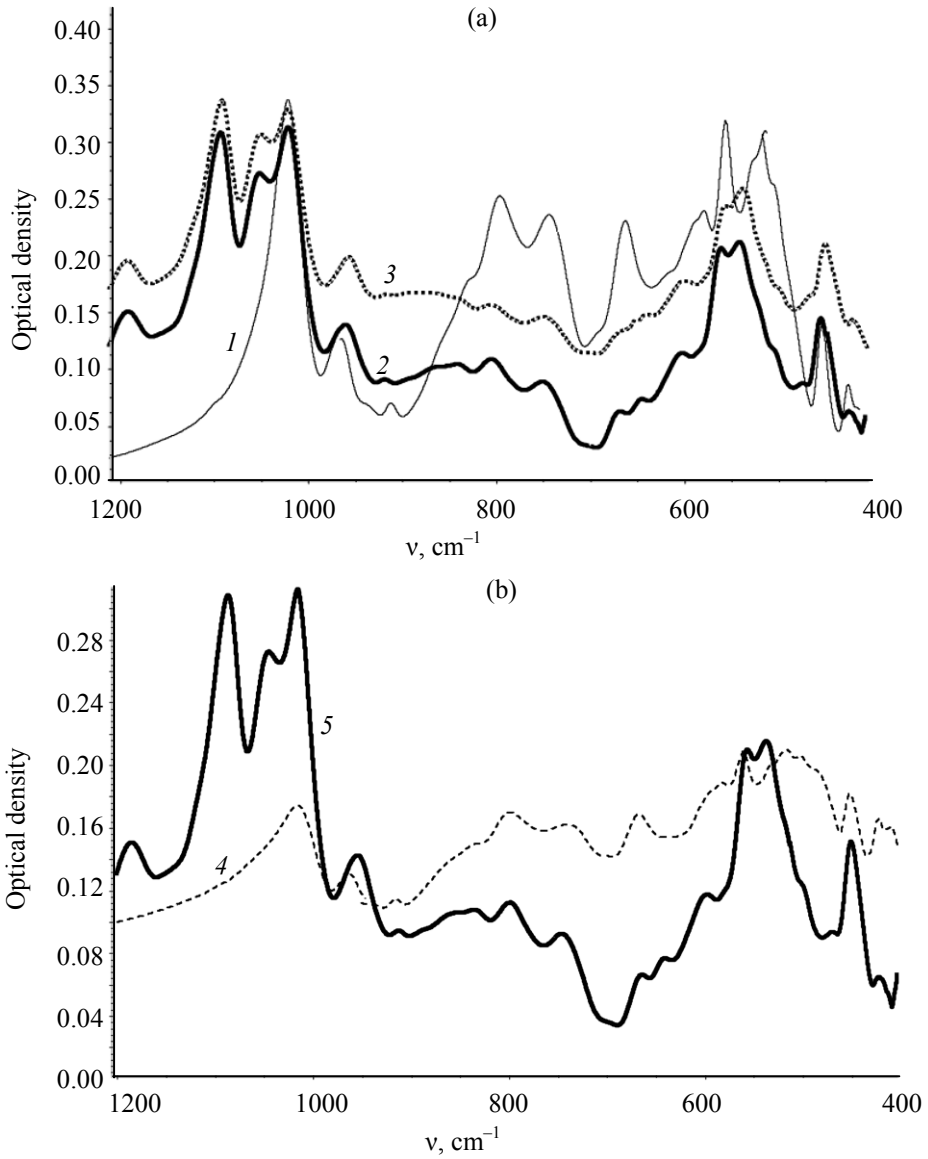

Fig. 9. IR spectra of gibbsite and products of its treatment with phosphate solutions. (a): (*1*) Gibbsite, H_2O, 2 months (control); phosphate concentration, M: (*2*) 1 (2 months), and (*3*) 2 (2 months). (b): Time of treatment with a 1 M phosphate solution: (*4*) 1 day and (*5*) 2 months.

The observation in the IR spectra (Fig. 8b) of P=O absorption bands points to the lack of symmetry in phosphate tetrahedra. The symmetry disturbance results from the coordination to aluminum atoms and the presence of protonated oxygen atoms. Stretching vibrations of coordinated P–O groups can be associated with the absorption bands at 1091 and 1050 cm^{-1} (Fig. 9a). The bands at 956 and 536 cm^{-1} are assignable to stretching and deformation vibrations of protonated P–O–(H) groups, and the bands at 800 and 1190 cm^{-1}, stretching and deformation vibrations of proton-acceptor (P)–O–H groups. The absorption bands at 900–800 and 650 cm^{-1} can be related to symmetric and antisymmetric stretching vibrations of P–O–P groups, characteristic of pyro(poly)phosphates. Note that the absorption intensity of these (and other P-containing) groups in gibbsite treated with a 2 M phosphate solution increases. The absorption bands near 600 and 540 cm^{-1} (Fig. 9a) belong to O–P–O groups [14, 34]. The fact that the IR spectra contain O–P–O and P–O–P bands suggests bi(poly)dentacity of ligands in the aluminophosphate complexes formed in gibbsite under treatment with 1 M and 2 M phosphate solutions.

As seen from Fig. 9b, already in the IR spectrum of gibbsite treated for 1 day with a 1 M phosphate solution one can observe absorption bands of O–P–O (600 and 480 cm^{-1}) and P–O–P (900–800 and ~650 cm^{-1}) groups. The vigorous dissolution of gibbsite in the corresponding solution (Figs. 2 and 6) is consistent with the formation of anionic complexes with bi(poly)dentate ligands.

Figure 10 shows the transformation sequence of anionic complexes under increasing phosphate loading of gibbsite. The absorption band at 398 cm^{-1} initially present in the IR spectrum of gibbsite (Fig. 10a, spectrum *1*) and assigned to the Al–O bond in anionic aquo(hydroxo) aluminum complexes disappears after 2-month treatment with a 10^{-3} M phosphate solution (spectrum *2*). Therewith, the band at 380 cm^{-1}, which, too, is associated with complex anions, increases in intensity and changes shape, and a P–O bond appears at the same position (410 cm^{-1}) as the shoulder in the control spectrum *1*. These changes can be explained by an incorporation of a monodentate anion $H_2PO_4^-$ into aluminum hydroxo complexes. Apparently, the fact that the new complexes had the same charge favored their retention in the solid phase, as evidenced by the enhanced intensity of all absorption bands in spectrum *2*. By contrast, all bands in spectrum *3* (Fig. 10a) had a lower intensity than in the reference spectrum *1*, on account of gibbsite dissolution in a 10^{-1} M phosphate solution (Figs. 1, 2). Consequently, treatment with this solution formed aluminophosphate complexes with a higher negative charge than in the case of a 10^{-3} M solution, and the resulting complexes passed into the liquid phase.

The IR spectrum of the product formed after 1-day treatment of gibbsite with a 1 M phosphate solution (Fig. 10b, spectrum *5*) contains absorption bands at 480, 418, and 390 cm^{-1} assignable to bidentate O–P–O groups. These bands disappeared from the IR spectrum of the product formed after 2-month treatment of gibbsite with a 1 M phosphate solution (Fig. 10c, spectrum *7*), probably, because of the dissolved anionic chelate aluminophosphate complexes.

The IR spectral patterns (Fig. 10c, spectra *7* and *8*) of the products formed after 2-month treatment of gibbsite with 1 M and 2 M phosphate solutionми, as compared with the reference spectrum *6*, showed that gibbsite vigorously dissolved in the corresponding solutions (Figs. 6 and 7) due to formation of soluble aluminum pyro(poly)phosphate complexes. Apparently,

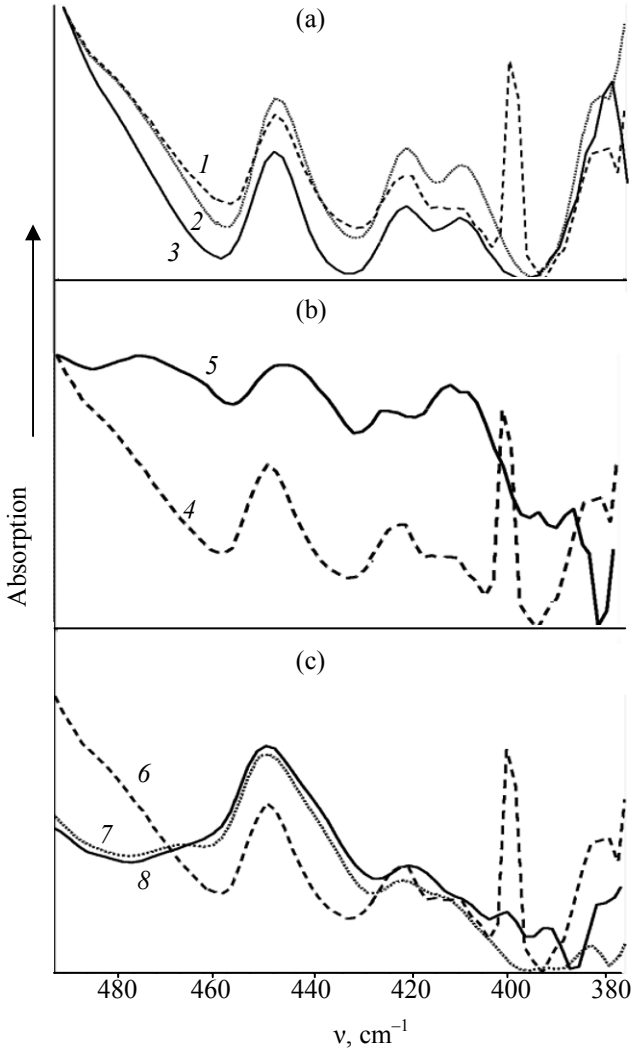

Fig. 10. IR spectra of gibbsite and products of its treatment with phosphate solutions. (a): (*1*) Gibbsite, H_2O, 2 months (control); phosphate concentration, M: (*2*) 10^{-3} (2 months) and (*3*) 10^{-1} (2 months). (b): (*4*) Gibbsite, H_2O, 2 months (control); phosphate concentration, M: (*5*) 1 (1 day). (c): (*6*) Gibbsite, H_2O, 2 months (control); phosphate concentration, M: (*7*) 1 (2 months) and (8) 2 M (2 months).

the new absorption bands at 400–375 cm^{-1} (spectra *7* and *8*) were associated with such complexes.

The revealed sequential structural transformations in anionic aluminum complexes with increasing phosphate loading of gibbsite can be illustrated by the following scheme:

$$Al(OH)_3 \rightarrow [Al(OH)_4]^- \rightarrow [Al(OH)_3(H_2PO_4)]^-$$
$$\rightarrow [Al(OH)_2(H_2PO_4)_2]^- \rightarrow [Al(OH)_2(H_2PO_4)(HPO_4)]^{2-}$$
$$\rightarrow [Al(OH)_2(HPO_4)_2]^{3-} \rightarrow [Al(OH)_2(HPO_4)(PO_4)]^{4-}$$
$$\rightarrow [Al(OH)_2(HPO_4)(P_2O_7)]^{5-} \rightarrow [Al(OH)_2(PO_4)(P_2O_7)]^{6-}$$
$$\rightarrow [Al(OH)_2(P_2O_7)_2]^{7-}.$$

As follows from the scheme, the value of the negative charge of aluminophosphate complexes depends on the number of coordinated H_2PO_4 ligands and their deprotonation. The highest negative charge is characteristic of the complexes with ligands containing P–O–P groups. The appearance of such groups can be explained by the addition of phosphate anions from the solution to the P atoms in the bidentate O–P–O groups coordinated to aluminum. The theoretical explanation of the mechanism of development of the effective positive charge on the P atom with references to original works is given in [35]. The P–O–P groups characteristic of pyro(poly)phosphates were found in the structure of phosphate minerals (lithogenic and biogenic) [36–38]. It can be suggested that polyphosphates play a certain role in mineral formation processes.

The possibility of reactions at positively polarized ligand P atoms in aluminophosphate complexes is an essential (and previously never considered) mechanism of binding of phosphate anions. According to our data, this mechanism is responsible for the enhancement of gibbsite dissolution processes and taranakite formation in the systems containing 1 M and 2 M phosphate solutions, where there are conditions for formation of anionic aluminum complexes with pyro(poly)phosphate ligands.

The formation of such complexes is confirmed by the analysis of the crystalline precipitate in the liquid phase of the gibbsite–1 M phosphate solution system after 3-month storage at room temperature. The XRD pattern of the precipitate [2] is more likely assignable to ammonium and aluminum pyrophosphates than to $NH_4H_2PO_4$ in the solution used for treatment of gibbsite (no precipitate formed in this solution after storage in similar conditions). The IR spectrum of the precipitate contained bands in the range 600–800 cm^{-1} supportive of the presence of P–O–P bonds in the structure. According to the reference data in [31], the corresponding bands are observed in the IR spectra of ammonium and aluminum ammonium salts of pyrophosphoric acid, as well as in ammonium taranakite with a standard chemical formula and are absent in the IR spectra of ammonium orthophosphates [$NH_4H_2PO_4$ and $(NH_4)_2HPO_4$].

Spectrometric analysis showed that the crystal contained 21.46(0.4)–24.26(0.7)% of phosphorus, 14.80(0.7)–16.91(0.5)% of nitrogen, and 0.77(0.1)–3.29(0.3)% of aluminum. The scatter of data for 5 points on the surface gave evidence for the presence of different complexes associated with each other. The closeness of the average P/N ratio (1.44) to that for $(NH_4)_3HP_2O_7$ (1.48) (Table 2) and the presence of aluminum in the product suggests that the matrix anionic aluminum pyro(poly)phosphate complexes associated individual components of the liquid phase, including NH_4^+ cations. Apparently, in view of the fact that their ligands are ably to adopt configurations convenient for ring closure, aluminum pyro(poly)phosphate complexes favor formation of the crystal phase (i.e. showed a template effect).

The key role in ring closure and crystal formation belongs to hydrogen bonds [39]. Having proton-donor and proton-acceptor P-containing groups, the pyro(poly)phosphate ligands can form hydrogen bonds of different strengths with the NH and OH groups of solution components [14]. The data in Table 3 provide evidence to show that hydrogen bonds present both in the crystalline precipitate formed in the liquid phase of the gibbsite−1 M phosphate solution and in ammonium taranakite.

The hydrogen bonds involving NH and OH groups absorb at 3100–2600 (2000) cm^{-1} [34, 40]. The larger the low-frequency shift, the stronger the hydrogen bond. The hydrogen bonds involving the P(O)OH group which can function both as a proton donor (P–O–H) and a proton acceptor (P=O oxygen) are stronger [14]. Protic donor−acceptor interactions in this group stabilize chelate aluminophosphate complexes. Phosphorus-containing groups can function as intermolecular linkers ensuring formation of macromolecules. As judged from the positions of the absorption maxima in the IR spectra (Table 3), the hydrogen bonds involving proton-donor P–O–(H) and proton-acceptor (P)–OH groups in ammonium taranakite were stronger than the respective bonds in the precipitate in the liquid phase, probably, due to a greater number of chelate aluminum complexes with polyphosphate ligands in the former.

According to the resulting data, ammonium taranakite as a system of aluminum complexes is a result of self-organization via formation of strong metal–ligand coordination bonds and multiple (highly directional and long-distant [41]) hydrogen bonds between polydentate phosphate ligands and solution components, in particular, ammonium ions. As mentioned above (Fig. 7, Table 1), the shape and size of ammonium taranakite crystals depends on their nitrogen content. Analogous data are reported in [13]. Apparently, hydrogen bonds

Table 3. IR absorption maxima of hydrogen bonds, cm^{-1}

Band assignment	Product from the liquid phase of the system gibbsite–1 M phosphate solution	Product of gibbsite treatment with phosphate solution (ammonium taranakite)	
		1 M	2 M
ν(NH)	3126.2	3129.3	3135.4
ν(OH)	2385.9	2430.1	2433.1
ν[P–O–(H)]	1020.1	956.1	953.8
δ[P–O–(H)]	549.1	536.5	538.9
ν[(P)–OH]	921.1	867.7	881.3
δ[(P)–OH]	1292.0	1189.6	1190.2

involving ammonium NH groups and their number and positions contribute, to a certain extent, to the morphological characteristics of ammonium taranakite crystals.

The importance of hydrogen bonds is evidenced by the fact that such bonds are found in the structures of natural and synthetic taranakites and their analogs [42–44]. In whole, the structure of taranakites cannot be considered established in view of the differences in the reported chemical compositions and conditions of synthesis [13, 25, 26, 28, 33, 42]. In our research we used the reference data [31] for the synthesized ammonium taranakite with the above-mentioned standard chemical formula calculated for two types of orthophosphate ligands in aluminum complexes. According to [33, 43], at least three types of complexes in taranakites have an octahedrally coordinated aluminum (coordination number 6). These data are better consistent with our results in favor of the importance of polyphosphate complexes.

According to [35], the synthesized ammonium taranakite contains two types of ligand phosphate groups in aluminum complexes. The phosphate groups of the first type contain a protonated O atom and in the phosphate groups of the second type the O atom is a hydrogen-bond acceptor. The different phosphate groups give two resonance signals in the ^{31}P NMR spectra at 5.7 and –18.5 ppm, respectively. Signals with similar chemical shifts (4.5 and –18.0 ppm) were also observed in the ^{31}P NMR spectra of the natural and synthesized potassium taranakites [43]. There is a suggestion that the first signals belong to the protonated orthophosphate group (P–O–H) in a monodentate anion $H_2PO_4^-$. However, this suggestion is inconsistent with the standard formula of taranakites with a protonated bidentate ligand HPO_4, as well as with our data showing that ammonium taranakite was formed by anionic aluminum complexes with both bi- and polydentate ligands which, too, can contain protonated groups. The second (predominant) signals are assignable to proton-acceptor P=O groups which can also belong to condensed phosphates [45, 46].

Taranakites are most commonly synthesized under heating. As the temperature increases, the δ_{31} of the proton-acceptor P=O groups in the ^{31}P NMR spectra of taranakites shifts to more negative values [3, 43], probably, due to the dehydration-induced polymerization of phosphate tetrahedra. As shown in [12], the rate of binding of phosphate anions with gibbsite decreased with increasing temperature; simultaneously, decomposition of gibbsite crystals was observed. These data agree with our results in two principal points. First, they provide evidence for the possibility of transfer of the formed aluminophosphate complexes into the liquid phase (dissolution of phosphatized gibbsite). Second, the fact that the process accelerated with temperature suggests an polyphosphate nature of ligands in the soluble complexes.

Taranakites can also be synthesized at room temperature, provided the reaction medium contains more phosphorus than aluminum [33, present work]. When aluminum in the phosphate system is contained in the solid phase (gibbsite), the rate of its release is a factor that limits taranakite formation [47]. As shown above, the rate of aluminum release from gibbsite increased with increasing concentration of $NH_4H_2PO_4$ solution, i.e. it was dependent of the type of aluminophosphate complexes that form. Taranakite formed at concentrations of 1 M and 2 M P, specifically, under conditions favoring condensation of phosphate tetrahedra. In [47], ammonium taranakite formed when gibbsite was treated with a saturated solution of

$NH_4H_2PO_4$, which initially contained a certain amount of condensed phosphates [48]. The fact that the solubility of gibbsite increases in the presence of polyphosphates can be explained by the strong solubilizing effect underlain by their ability to form soluble chelate complexes with metals [19, 49].

According to the resulting data, the main factor responsible for transformation of gibbsite into taranakite is the presence in the phosphate solution of polyphosphates to drive the gibbsite dissolution process.

CONCLUSIONS

The data obtained in the present work can much refine our understanding of the processes that occur on the surface of the gibbsite mineral and involve phosphate anions from $NH_4H_2PO_4$ solutions. It was shown that complete binding of phosphate anions incorporated in aluminophosphate complexes retained on the surface took place only if the phosphate solutions had concentrations close to those of natural soil solutions (10^{-6}–10^{-4} M). At higher phosphate concentrations characteristic of soil overphosphatized due to human activities (10^{-3}–1 M), phosphate anions were bound as soluble anionic aluminophosphate complexes. The negative charge of the complex anions increased with increasing phosphate loading on the sorbent, as evidenced by the amount of the NH_4^+ ion retained on the phosphatized gibbsite surface. As the phosphate loading increased to 1 M, along with the dissolution of the phosphatized gibbsite layer, a surface coating consisting of a phosphate mineral, ammonium taranakite, with the phosphorus, aluminum, and nitrogen contents corresponding to a standard formula, forms. In the system gibbsite−2 M phosphate solution, bulk destruction of gibbsite crystals takes place, and they are replaced by ammonium taranakite crystals with increased phosphorus and nitrogen contents. It is suggested that the enhanced dissolution of gibbsite accompanied by taranakite formation is associated with intracomplex transformation of bidentate orthophosphate ligands into pyro(poly)phosphate. By forming multiple hydrogen bonds with solution components (including ammonium ions), polyphosphate ligands ensured association of different aluminophosphate complexes into a uniform crystal structure.

REFERENCES

1. Kudeyarova, A.Yu., *Ekol. Khim*., 2009, vol. 18, no. 4, pp. 202–221.
2. Kudeyarova, A.Yu. and Alekseeva, T.V., *Agrokhim.,* 2012, no. 2, pp. 27–38.
3. Lookman, R., Grobet, P., Merckx, R., and Van Riemsdijk, W.H., *Geoderma*, 1997, vol. 80, pp. 369–388.
4. Nanzyo, M., *J. Soil Sci*., 1984, vol. 35, no. 1, pp. 63–69.
5. Pierzynski, G.M., *Crit. Rev. Environ. Control*, 1991, vol. 21, nos. 3–4, pp. 265–295.
6. Van Emmeric, T.J., Sandstrom, D.E., Antzutkin, O.N., Angove, M.J., and Johnson, B.B., *Langmuir*, 2007, vol. 23, no. 6, pp. 3205–3213.
7. Grinberg, A.A., *Vvedenie v khimiyu complexnykh soedinenii* (Introduction to the Chemistry of Complex Compounds), Leningrad: Khimiya, 1971.
8. Laverdiere, M., *Can. J. Soil Sci*., 1982, vol. 62, pp. 519–525.
9. Bolan, N.S. and Barrow, N.J., *J. Soil Sci*., 1984, vol. 35, no. 2, pp. 273–281.
10. Del Nero, M., Galindo, C., Barillon, R., Halter, E., and Made, B., *J. Colloid Interface Sci*., 2010, vol. 342, no. 2, pp. 437–444.
11. Ryden, J.C., McLaughlin, J.R., and Syers, J.K., *J. Soil Sci*., 1977, vol. 28, no. 1, pp. 72–92.
12. Van Riemsdijk, W.H., and Lyklema, J., *J. Colloid Interface Sci*., 1980, vol. 76, no. 1, pp. 55–66.
13. Wei, L., Ye, S., Tian, Y., Xie, Y., and Chen, Y., *J. Cryst. Growth*, 2009, vol. 311, pp. 3359–3363.
14. Corbridge, D.E.C. and Corbridge, D.E., *Phosphorus: An Outline of Its Chemistry, Biochemistry, and Technology*, Amsterdam: Elsevier, 1980.
15. *The Chemistry of the Coordination Compounds*, Bailar, J.C . Jr . and Busch, F. O., Eds., New York: Reinhold, 1956. Translated under the title *Khimiya koordinatsionnykh soedinenii*, Moscow: Inostrannaya Literatura, 1960, pp. 7–86.
16. *Phosphorus and Its Compounds*, *vol. 1: Chemistry*, Van Wazer, J.R., Ed., New York: Interscience, 1958.
17. Lapina, L.M. and Grishina, I.A., *Mineral'nye udobreniya i sernaya kislota* (Mineral Fertilizers and Sulfuric Acid), Moscow: NIUIF, 1973, vol. 221, pp. 56–62.
18. Kudeyarova, A.Yu. and Kvaratskheliya, M.Z., *Pochvoved.*, 1989, no. 8, pp. 26–34.
19. Kudeyarova, A.Yu., *Pedogeokhimiya orto- i polifosfatov v usloviyakh primeneniya udobrenii* (Pedogeochemistry of Ortho- and Polyphosphates Under Fertilizer Use Conditions), Moscow: Nauka, 1993.
20. Kudeyarova, A.Yu. and Trubin, A.I., *Pochvovedenie*, 1976, no. 11, pp. 108–118.
21. Wang, H.D., Harris, W.G., and Yuan, T.L., *Soil Crop Sci. Soc. Fla. Proc*., 1989, vol. 48, pp. 49–55.
22. Wilson, M.J. and Bain, D.C., *Am. Miner*., 1976, vol. 61, pp. 1027–1028.

23. Qureshi, R.H., Jenkins, D.A., and Davies, R.I., *Soil Sci. Soc. Am. J.,* 1978, vol. 42, no. 5, pp. 698–703.
24. Simas, F.N.B., Schaefer, C.E.G.R., Melo, V.F., Albuquerque-Filho, M.R., Michel, R.F.M., Pereira, V.V., Gomes, M.R.M., and Da Costa, L.M., *Geoderma*, 2007, vol. 138, pp. 191–203.
25. Sakae, T., and Sudo, T., *Am. Miner*., 1975, vol. 60, pp. 331–334.
26. Fiore, S., Laviano, R., *Am. Miner*., 1991, vol. 76, pp. 1722–1727.
27. Willems, L., Compere, Ph., Hatert, F., Pouclet, A., Vicat, J.P., Ek, C., and Boulvain F., *Terra Nova*, 2002, vol. 14, no. 5, pp. 355–362.
28. Landis, C.A., and Craw, D., *J. Royal Soc. New Zealand*, 2003, vol. 33, no. 1, pp. 487–495.
29. Mikheev, V.I., *Rentgenometricheskii opredelitel' mineralov* (X-ray Detector of Minerals), Moscow: Gosgeoltekhizdat, 1957.
30. Arinushkina, E.V., *Rukovodstvo po khimicheskomu analizu pochv* (Manual on the Chemical Analysis of Soils), Moscow: Mosk. Gos. Univ., 1970.
31. Lehr, J.R., Brown, E.H., Frazier, A.W., Smith, J.P., and Thrasher, R.D., *Crystallographic Properties of Fertilizer Compounds,* Muscle Shoals, AL: National Fertilizer Development Center, 1967.
32. Nriagu, J.O*., Can. J. Earth Sci*., 1976, vol. 13, no. 6, pp. 717–736.
33. Schwieger, W., Meyer zu Altenschildesche, H., Kokotailo, G.T., and Fyfe, C.A., *Z. Anorg. Allg. Chem*., 1998, vol. 624, pp. 1712–1717.
34. Nakamoto, K., *Infrared and Raman Spectra of Inorganic and Coordination Compounds*, New York: Wiley, 1963.
35. Kudeyarova, A.Yu., *Pochvoved.*, 2007, no. 9, pp. 1048–1063.
36. Kislovskii, L.D., Knubovets, R.G., and Cherenkova, G.I., *Dokl. Akad. Nauk SSSR*, 1977, vol. 232, no. 3, pp. 581–583.
37. *Issledovanie fosfatov kal'tsiya fizicheskimi metodami* (Study of Calcium Phosphates by Physical Methods), Gilinskaya, L.G., Ed., Novosibirsk: Nauka, 1979.
38. Le Geros, R.Z. and Le Geros, J.P., *Phosphate Minerals*, Berlin: Springer, 1984, pp. 351–385.
39. Steed, J.W. and Atwood, J.L., *Supramolecular Chemistry*, New York: Wiley, 2000. Translated under the title *Supramolekulyarnaya khimiya*, Moscow: Akademkniga, 2007, vol. 1.
40. Bellami, L., *The Infrared Spectra of Complex Molecules*, London: Butterworths, 1960.
41. Steed, J.W. and Atwood, J.L., *Supramolecular Chemistry*, New York: Wiley, 2000. Translated under the title *Supramolekulyarnaya khimiya*, Moscow: Akademkniga, 2007, vol. 2.
42. Frost, R.L., Xi, Y., Palmer, S.J., and Pogson, R.E., *Spectrochim. Acta, Part A*, 2011, vol. 83, no. 1, pp. 106–111.
43. Bleam, W.F., Pfeffer, P.E., and Frye, J.S*., Phys. Chem. Miner*., 1989, vol. 16, no. 8, pp. 809–816.
44. Dick, S. and Zeiske, T., *Z. Naturforsch B*, 1998, vol. 53, pp. 711–719.
45. Newman, R.H. and Tate, K.R., *Commun. Soil Sci. Plant Anal*., 1980, vol. 11, no. 9, pp. 835–842.
46. Condron, L.M., Goh, K.M., and Newman, R.H., *J. Soil Sci*., 1985, vol. 36, no. 2, pp. 199–207.
47. Beaton, J.D., Bryan, J.M., Russell, J.C., and Speer, R.C*., Nature*, 1964, vol. 201, no. 4920, pp. 739–740.
48. *Analiticheskaya khimiya fosfora* (Analytical Chemistry of Phosphorus), Lyalikov, Yu.S., Moscow: Nauka, 1974.
49. Kudeyarova, A.Yu. and Kvaratskheliya, M.Z., *Geoderma*, 1984, vol. 34, pp. 251–259.